View metadata, citation and similar papers at core.ac.uk
brought to you by CORE
provided by OceanRep

The Impact of Data Assimilation on ENSO Simulations and Predictions

MARTIN FISCHER AND MOJIB LATIF

Max-Planck-Institut für Meteorologie, Hamburg, Germany

MORITZ FLÜGEL

Texas A&M University, College Station, Texas

MING JI

National Centers for Environmental Prediction, Washington, D.C.

(Manuscript received 16 June 1995, in final form 24 May 1996)

ABSTRACT

In this study, the impact of oceanic data assimilation on ENSO simulations and predictions is investigated. The authors' main objective is to compare the impact of the assimilation of sea level observations and three-dimensional temperature measurements relative to each other. Three experiments were performed. In a control run the ocean model was forced with observed winds only, and in two assimilation runs three-dimensional temperatures and sea levels were assimilated one by one. The root-mean-square differences between the model solution and observations were computed and heat content anomalies of the upper 275 m compared to each other. Three ensembles of ENSO forecasts were performed additionally to investigate the impact of data assimilation on ENSO predictions. In a control ensemble a hybrid coupled ocean–atmosphere model was initialized with observed winds only, while either three-dimensional temperatures or sea level data were assimilated during the initialization phase in two additional forecast ensembles. The predicted sea surface temperature anomalies were averaged over the eastern equatorial Pacific and compared to observations. Two different objective skill measures were computed to evaluate the impact of data assimilation on ENSO forecasts.

The authors' experiments indicate that sea level observations contain useful information and that this information can be inserted successfully into an oceanic general circulation model. It is inferred from the forecast ensembles that the benefit of sea level and temperature assimilation is comparable. However, the positive impact of sea level assimilation could be shown more clearly when the forecasted temperature differences rather than the temperature anomalies themselves were compared with observations.

1. Introduction

The strongest signal on the short-range climatic timescale is the El Niño–Southern Oscillation phenomenon (ENSO). It is characterized by a weakening of the trade winds along the equator and a huge redistribution of heat from the western to the eastern tropical Pacific. The impacts of ENSO are felt worldwide through a disruption of the atmospheric general circulation pattern (Ropelewski and Halpert 1987), which leads, for instance, to severe droughts in northwest Australia and southeast Asia during an El Niño event. The northeast region of Brazil and Zimbabwe are other regions where rainfall variations are highly correlated with ENSO indices and there are many other examples. Off the Peruvian coast, the marine ecosystem is directly affected by the oceanic variations in upwelling, which has a large impact on fishing. For all these regions, reliable ENSO forecasts would offer decision-makers an opportunity to take account of anticipated climate variations, in order to reduce impacts of ENSO on the economy. Thus, it is a logical consequence that the study of ENSO predictability has become a field of major research. ENSO can be regarded as a slow oscillation of the coupled ocean–atmosphere system. However, it is commonly believed that the memory (or inertia) of the system resides entirely in the upper few hundred meters of the ocean (e.g., Wyrtki 1985). According to the theory of the *delayed action oscillator* (Schopf and Suarez 1988) the evolution of warm and cold events is determined by the propagation of equatorial waves and their reflection at the meridional boundaries, which implies that ENSO is inherently predictable on timescales up to a few years.

Since ENSO is a phenomenon of the coupled system, coupled ocean–atmosphere models are required for its prediction. Such models have been developed over the

Corresponding author address: Dr. Martin Fischer, Max-Planck-Institut für Meteorologie, Bundestrasse 55, 20146 Hamburg, Germany.
E-mail: martin.fischer@dkrz.de

© 1997 American Meteorological Society

last 10 years by different groups and applied to ENSO forecasts (e.g., Cane et al. 1986; Barnett et al. 1988; Leetmaa and Ji 1989; Latif et al. 1994). ENSO forecasting is an initial value problem, that is, the further evolution of the system depends highly on the initial state from which it started. This is at least valid over a certain time, which is called the predictability time. Although ENSO is a phenomenon of the coupled system, its evolution is determined mainly by the ocean. Therefore, the initialization can be considered as an initial value problem for the ocean. Thus, a very important task in carrying out an ENSO forecast is to determine the oceanic initial state as accurately as possible.

One very common way to initialize an ENSO forecast with a coupled ocean–atmosphere model is as follows. The oceanic model is integrated in an uncoupled mode and forced by observed wind stresses and heat fluxes, which yield the initial state from which the coupled model prediction is started. Errors in the initial state are due to forcing errors, in particular wind stress forcing, and errors in the model formulation. This can be compensated for partly by inserting additional, independent information into the model during the initialization phase. The most promising approach is to assimilate oceanic subsurface information, to get a more realistic initial state. Recently, different groups have shown that assimilation of subsurface temperature observations may lead to improved forecasts (Ji and Leetmaa 1997; Kleeman et al. 1995). However, the distribution of these data in space and time is quite irregular and sometimes very sparse. Especially in the central Pacific, only very few observations are available (Levitus and Gelfeld 1992). An alternative data type is given by sea level observations. Variations of the subsurface density structure, which are crucial for the evolution of El Niño events, lead to corresponding changes in sea level. It is a good approximation for the tropical oceans to assume that the relation between density and sea level variations is linear. Further, we may neglect salinity variations, which leads to a linear relation between changes in the vertical temperature structure and sea level. From this we may infer that sea level observations in the Tropics contain important information about the vertical temperature structure of the tropical oceans.

In contrast to numerous studies about the assimilation of sea level data for oceanic circulation studies, this is an attempt to explore the impact of sea level assimilation on coupled model ENSO predictions. In a control prediction ensemble, the model is initialized by observed wind forcing only. In the other two ensembles, observations are assimilated additionally. In one case, we assimilate subsurface temperature data, and in the other case sea level anomalies. The predictive skills obtained from the three ensembles are compared to each other. Our main focus is the question to which extent sea level data contain sufficient information about the vertical density structure to replace the subsurface in situ measurements. This is an important issue, since altimetric sea levels from recently launched satellites appear to be rather reliable (Busalacchi et al. 1994), and the satellites provide information with very high spatial and temporal resolution. The paper is organized as follows. In section 2, we present our forecast system and in section 3 a short description of the data we used is given. In section 4, we describe the ocean model integrations that were conducted with and without data assimilation. In section 5, we describe the results of the ENSO forecasts that were performed from different initial ocean states. The conclusions are stated in section 6.

2. The forecast system

Our forecast system consists of two major parts: a coupled ocean–atmosphere model and an ocean assimilation system. In the following subsections, brief descriptions of the coupled model and the data insertion method are given. Special emphasis is put on the empirical scheme used to assimilate sea level anomalies into our oceanic primitive equation model.

a. The coupled model

The coupled model consists of an oceanic general circulation model coupled to a statistical atmospheric feedback model. The ocean model was primarily developed to investigate the El Niño–Southern Oscillation phenomenon in the tropical Pacific and is a further development of the model described by Latif (1987). It is a limited domain, primitive equation model extending from 130°E to 80°W in the zonal direction and from 30°S to 30°N in the meridional direction. The eastern and western coast lines are realistic, while the northern and southern boundaries are closed. The bottom is assumed to be flat at a constant depth of 4000 m. The hydrostatic and the Boussinesq approximations are used but no rigid lid is assumed; that is, the sea level height is a prognostic variable in our model. In this model, salinity is not considered, which is a reasonable approximation for the Tropics. The zonal resolution is about 6°. In the meridional direction, the resolution decreases from 0.5° at the equator to about 4° at the northern and southern boundaries. The model has 13 levels in the vertical, with 10 levels placed in the upper 300 m. The horizontal eddy viscosity is assumed to be constant at a value of 10^8 cm^2 s^{-1}, while no explicit horizontal heat diffusion is included. The vertical mixing coefficients are Richardson number dependent (Pacanowski and Philander 1981). A time step of 2.25 h is used. The model is forced by observed monthly mean wind stress fields (FSU product; Goldenberg and O'Brien 1981; Legler and O'Brien 1984), and a Newtonian cooling type heat flux formulation (Haney 1971) with a relaxation time of 30 days toward an *equivalent* observed climatological temperature is applied. A detailed description of the model performance is given in Latif (1987) and Barnett et al. (1993). We assume that

the memory of the coupled ocean–atmosphere system resides entirely in the tropical Pacific. It is therefore possible to use a *minimum* atmospheric model with no internal dynamics, which passively responds to the anomalous boundary conditions provided by the ocean. Further, we assume a linear relation between the dominant anomaly patterns of sea surface temperature and wind stress. In the following, we explain how the atmosphere model was constructed (see also Barnett et al. 1993). We decompose observed sea surface temperature $T'(x, t)$ and wind stress anomalies $\tau'(x, t)$ into empirical orthogonal functions (EOF):

$$T'(x, t) = \sum_{n=1}^{N} \alpha_n(t)E_n(x) \tag{1}$$

$$\tau'(x, t) = \sum_{n=1}^{N} \beta_n(t)F_n(x). \tag{2}$$

Here, α_n and β_n are the principal components and E_n and F_n are the spatial patterns, respectively. A matrix of regression coefficients $\mathbf{C}$ relating the two vectors of principal components is obtained by minimizing the function

$$\langle(\mathbf{C}\boldsymbol{\alpha} - \boldsymbol{\beta})^2\rangle, \tag{3}$$

where angle brackets denote the time expectation operator. During a coupled model run the actual wind stress anomaly field is computed as follows. From the SST anomalies, the corresponding principal components are computed by projection onto the corresponding EOFs,

$$\alpha_n(t) = \sum_{x} T'(x, t)E_n(x), \tag{4}$$

from which the principal components for the EOF expansion of the wind stress anomaly fields are determined as

$$\beta_n = \sum_{m=1}^{N} C_{nm}\alpha_m, \tag{5}$$

which are finally inserted into Eq. (2). The leading five EOFs were retained for the prediction experiments. To obtain self-sustained oscillations in a coupled control run, the wind stress anomalies computed with the statistical model were scaled by a factor of 1.4, and this factor is applied to all coupled experiments described below. The performance of the ocean model as measured by its ability to reproduce the observed SST in response to prescribed observed wind stresses is good but not perfect. This means that the ocean model SSTs passed to the statistical atmosphere differ in some respect from those that were used to develop the atmosphere. This error was corrected by constructing an interface between the ocean and the atmosphere model (Barnett et al. 1993). Again, a regression approach was used, by which the relation between the simulated and observed SST patterns was approximated. The leading five EOFs of the observed and simulated SST anomalies (obtained from a run forced with observed wind stress fields) were used to derive the *correction matrix*. The interface or *correction matrix* was constructed similarly to the regression matrix $\mathbf{C}$, described above. The simulated SST anomalies are corrected by this interface before they are passed to the statistical atmosphere model.

The coupled model simulates a regular ENSO cycle with a period of approximately five years, which was inferred from a multidecadal control run.

b. The assimilation scheme

1) THE INSERTION TECHNIQUE

We use a continuous data assimilation scheme, that is, the model solution is updated every time step. Two components are required, a spatial analysis system and a method to spread information in time. The spatial objective analysis technique is based on the successive correction method (Daley 1991). The analyzed field is obtained from a background or first guess field by adding a linear combination of all deviations between the observations and first guess:

$$[f_A]_i = [f_B]_i + \frac{\sum_k E_O^{-2}W_{ik}[f_O - f_B]_k W_t}{E_B^{-2} + \sum_k E_O^{-2}W_{ik}W_t}F \tag{6}$$

with

$$W_{ik} = \exp\left[-\frac{(x_i - x_k)^2}{L_x^2} - \frac{(y_i - y_k)^2}{L_y^2}\right] \tag{7}$$

and

$$W_t = \begin{cases} 1 - \dfrac{|t - t_0|}{\delta t}, & |t - t_0| < \delta t \\ 0, & |t - t_0| \geq \delta t \end{cases}. \tag{8}$$

Model grid points are indexed by an i, observational points by a k. Here, $[f_A]$ are the analyzed values of a field, $[f_B]$ the corresponding background or first guess field, and $[f_O]$ the observations. When assimilating data into a model, the first guess is provided by the model itself. Here, $E^2_{O/B}$ are the estimated error variances of the observations and the background, respectively. Every increment between first guess and observed value is multiplied by a time weight W_t, which increases linearly from zero to one and back to zero, as the difference between model time and observational time goes from $t_0 - \delta t$ to zero and to $t_0 + \delta t$. The time weight acts as a temporal filter reducing the effects of high-frequency variability in the data, which are not resolved by our model. Further, the observational increments are weighted with the background error correlation. Because these correlations are not exactly known, they must be estimated. Here, we assume that the correlations are only a function of the distance between points and not of their absolute position. We chose a Gaussian shape func-

tion with different characteristic *e*-folding scales L_x and L_y in the zonal and meridional direction [Eq. (7)]. Finally, the obtained correction is multiplied by a constant factor F. This factor determines how fast the data are inserted into the model. If we assume that the spatial weights and the error variances are equal to one, and that E_B^{-2}/E_O^{-2} is an order of magnitude larger than W_t, then Eq. (6) is the discretized version of the differential equation $\partial f/\partial t = F'W_t(f_o - f)$, where $F' = F/\Delta t$ and Δt is the time step. If W_t increases linearly from zero to one over a time interval δt, then the characteristic *e*-folding time of this equation is $t_{1/e} = (2\delta t\Delta t/F)^{1/2}$. With a time step of 2.25 h, a time window of 15 days, and $F = 0.1$, we obtain a relaxation time of about 4 days. Good results were obtained with relaxation times between 4 and 16 days, which corresponds to a range of F between 0.1 and 0.005. In all experiments described here, a factor of $F = 0.1$ was chosen.

The correction of the model solution is applied every time step to ensure that the corrections remain small, so that the balance between the velocity and mass fields is disturbed only slightly. This is important to avoid the generation of high-frequency gravity waves. Thus, no normal mode initialization is necessary. After each correction step a convective adjustment routine is applied to remove unstable stratification.

In all assimilation experiments presented below, the *e*-folding scales for the spatial weights were set to 1000 km in the zonal and 200 km in the meridional direction. The half-width of the time window was 7.5 days, so that data within 15 days, centered on the actual model time step, were used. These parameters are the same for all depths. We assumed further that the error variance of the background field—that is, the model solution—is twice as large as that of the observations, so that more weight is given to the observations.

Our assimilation scheme is relatively simple. However, for large-scale studies in conjunction with gridded datasets, as in our case, it seems to be appropriate. For homogeneous data point distributions, which do not change with time, the successive correction method is equivalent to the optimal interpolation scheme that has been used extensively in operational weather prediction schemes.

2) How to use sea level observations

Although sea surface elevation is a prognostic variable in our model, it is not sensible to correct the sea surface height (SSH) directly. This would affect the barotropic mode only, and the information would be lost within a few time steps. Sea surface elevation is an integral quantity that contains information about the vertical density structure. To assimilate SSH observations, the information contained in the data must be transformed into a correction of the mass field. For the Tropics, a linear relation between small changes in sea level and the corresponding changes in the vertical mass structure is a reasonable assumption. Further, salinity variations can be neglected, which yields a linear relation between anomalies in the vertical temperature stratification and sea level. We correct, therefore, the vertical temperature structure only. The relationship between changes in sea level and those in the vertical temperature structure was derived empirically from a control run in which our ocean model was forced by observed winds over the period January 1982–December 1992. For every horizontal grid point, an EOF analysis of the anomalous vertical temperature profile was performed. Five EOFs were retained, explaining about 95% of the local variance in most of the model domain. Only very close to the horizontal boundaries (within one to two grid points) did the explained variances drop to about 65%, which we attribute to boundary effects. Regression coefficients A^n between SSH anomalies and the principal components γ of the EOFs $G_n(z)$ were computed and stored separately for every horizontal grid point. To insert the sea level observations into the model, first a correction field for the sea surface height anomalies $\Delta\zeta'$ was computed, applying the successive correction method. The principal components of the EOF expansion of the vertical temperature corrections are obtained by multiplying the sea level corrections by the A^n [Eq. (9)]. To obtain the desired temperature correction field, the principal components must be inserted into the EOF expansion of the anomalous temperature profile [Eq. (10)]:

$$(\gamma^n)_i = (A^n)_i(\Delta\zeta')_i, \tag{9}$$

$$[\Delta T'(z)]_i = \sum_{n=1}^{5} (\gamma^n)_i[G(z)^n]_i. \tag{10}$$

Finally, the temperature corrections were added to the first guess values, and a convective adjustment routine was applied to remove unstable stratifications. Thus, the surface height correction was transformed into a correction of the vertical temperature structure by applying the empirically derived relationship between anomalous sea surface height and vertical temperature structure. This was done separately for every grid point. The above described method is similar to that used by Mellor and Ezer (1991), with the exception that they did not project the sea level anomalies on EOFs but worked directly with temperature and salinity. In contrast, in our approach the sea level is indirectly changed. Using the leading EOFs only for the projection procedure ensures that the information is smoothed in the vertical and projected onto the dominant vertical mode of the model.

3. Data

The Florida State University (FSU) wind stress data (Goldenberg and O'Brien 1981; Legler and O'Brien 1984) were used to force the ocean model, and a relaxation of the temperatures in the uppermost ocean layer toward an *equivalent* observed climatological tem-

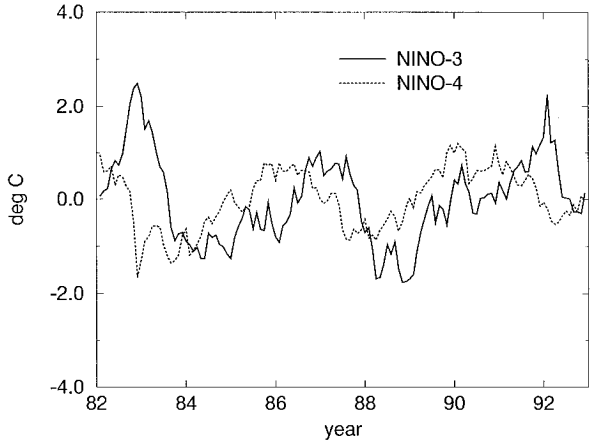

FIG. 1. Temperature anomalies averaged over the upper 275 m for Nino-3 and Nino-4, as derived from the NMC reanalysis. These indices are as upper-ocean heat content.

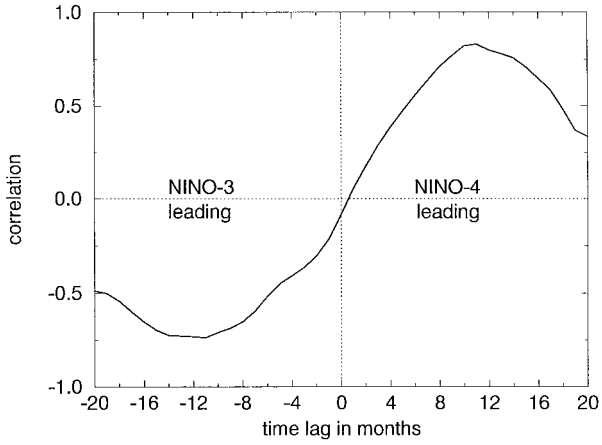

FIG. 2. Correlation between monthly mean heat content anomalies in Nino-3 and Nino-4 as a function of time lag between the two time series. A positive time lag means that the signal in Nino-4 is leading the signal in Nino-3. Data between January 1982 and December 1988 were used.

perature was applied. To validate the forecast experiments, predicted SST anomalies were compared to SST anomalies as obtained from the Reynolds dataset (Reynolds 1988; Reynolds and Smith 1994).

The assimilated data were obtained from the National Meteorological Center (NMC, now known as the National Centers for Environmental Prediction) reanalysis dataset. This is the output of an oceanic analysis system in which surface and subsurface temperature observations are assimilated into a high-resolution OGCM (Ji et al. 1995). The reanalysis provides a complete temperature and sea level analysis of the Pacific Ocean. We use these *pseudo data* instead of real observations, because one of the main objectives of this paper is to investigate the impact of different data types on ENSO predictions. The NMC reanalysis yields sea levels with the same resolution and comparable quality as temperatures. The temperatures and sea levels are the output of the same ocean model. Thus, they are dynamically consistent to each other and should contain the same information. This is a perfect condition to compare the impact of these two different data types on ENSO forecasts.

4. Ocean-only experiments

Three sets of experiments are presented. Each set consists of an initialization run with our ocean model, in which it is forced by observed wind stress fields, and an ensemble of forecast experiments conducted in coupled mode. No data were assimilated in the initialization run of the first set, which we use as our control experiment. In the second and third set, three-dimensional temperature and sea level anomalies were assimilated during the initialization runs, respectively. In the following subsections, we present some results obtained from the forced ocean model runs. Results from the forecast ensembles are presented in section 5.

a. Control run without data assimilation

The ocean model was integrated prescribing observed wind stresses from FSU (Goldenberg and O'Brien 1981; Legler and O'Brien 1984) for the period January 1982 to December 1992. The model is able to reproduce the observed temperature and sea level anomalies quite realistically. However, the maximum of the interannual SST variability is simulated too far in the west and too much confined to the equator (Fischer and Latif 1995). Since equatorial heat content variations are crucial to the ENSO cycle (Ji et al. 1994; Neelin et al. 1994), we compare in the following the heat content variations simulated by our model with those obtained from the NMC ocean reanalysis, which should be quite close to reality. We use as a measure of upper-ocean heat content the average of the temperatures over the upper 275 m, which was computed separately for the Nino-4 (5°N–5°S, 150°E–150°W) and Nino-3 (5°N–5°S, 150°–90°W) regions. As expected, all ENSO extremes observed during the period 1982–1993 can be clearly identified in the reanalysis (Fig. 1). However, it is more important in view of the ENSO predictability that there is a consistent phase shift between the heat content variations in the Nino-4 and those in the Nino-3 region. The signal in the western Pacific is leading by about one year. This can be seen more clearly in Fig. 2, showing the correlation between monthly mean heat content anomalies in Nino-3 and Nino-4 as a function of time lag. The correlations are based on the NMC reanalysis data for the period January 1982–December 1988, the period from which we initialized the forecast ensembles presented in section 5. The correlation function has a maximum at a lead time of eleven months, with a correlation of about 0.75, while the correlation is almost zero at zero lag. Thus, the heat content variations in the western Pacific can be regarded as a precursor for those in the

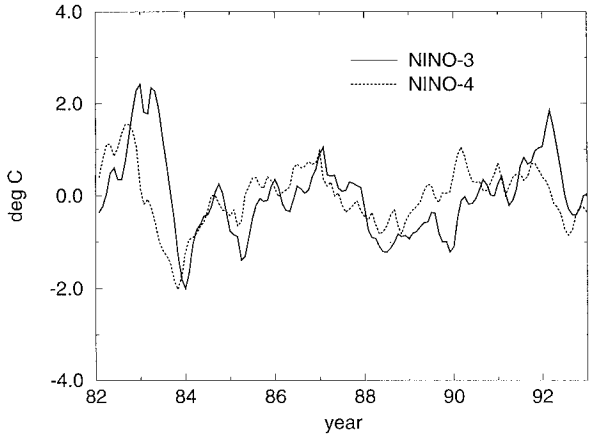

FIG. 3. Temperature anomalies averaged over the upper 275 m for Nino-3 and Nino-4 as derived from our ocean model forced by FSU wind stresses.

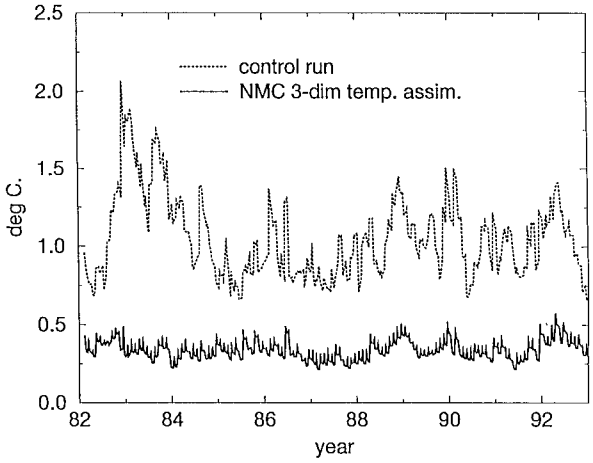

FIG. 4. Root-mean-square difference between simulated temperatures and NMC reanalysis Nino-4 temperatures for the period 1982–92.

eastern Pacific. The skill of an ENSO forecast system depends highly on its ability to simulate this precursor as accurately as possible. In Fig. 3, the same two heat content indices are shown as simulated in our control experiment without data assimilation. The main ENSO extremes are also simulated reasonably well in this control integration. However, the amplitude of the precursor is weaker than in the NMC reanalysis, and the phase lag between the Nino-3 and Nino-4 regions is less pronounced. The computation of the lag correlation yields a maximum of 0.75 at a lead time of about 5 months. Thereafter the correlation drops quickly and amounts to only 0.3 at a lead time of 12 months. The impact of these differences on the ENSO predictions is presented in section 5.

b. Assimilation of three-dimensional temperature anomalies

The model was again forced by observed monthly mean FSU wind stress fields, but now monthly mean three-dimensional temperature anomalies were assimilated during the period February 1982–December 1992. Overall, the model simulation was improved considerably, relative to the run without data assimilation. The maximum SST variability was shifted farther to the east, and the off-equatorial variability was enhanced (not shown). In the Nino-4 region, for example, the root-mean-square difference between the simulated temperature anomalies and those obtained from the NMC reanalysis was reduced by a factor of 3–4 relative to the control run (Fig. 4). Since the model simulations are compared to the same data that were assimilated, it is not surprising that a substantial reduction of the differences was achieved. However, this comparison gives an indication of the typical differences between model simulations and reality and the level of potential reduction. In Fig. 5, we display our measure for the upper-ocean heat content in the Nino-3 and Nino-4 region. The phase shift between the two time series is now very similar to that obtained from the NMC data, and it is more pronounced than in the control experiment (cf. Figs. 5, 1, and 3). Further, the amplitude of the precursor is stronger relative to the control run, so that a positive impact on the forecast skill can be expected. The amplitude of the interannual temperature variability was increased compared to both the control run and NMC data. This is surprising because the updated solution is a linear combination of the model solution and the assimilated data. One would expect, therefore, the amplitude of the variability to lie between that of the data and the control run. Only nonlinearities in the model can explain that behavior.

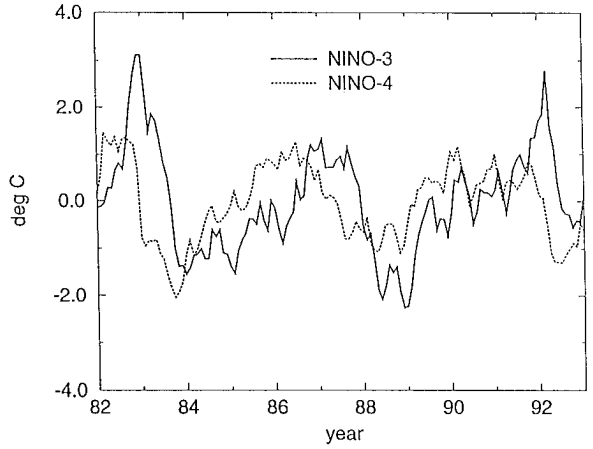

FIG. 5. Temperature anomalies averaged over the upper 275 m, as derived from the temperature assimilation run. The model was forced by observed wind stresses, and three-dimensional NMC temperatures were assimilated.

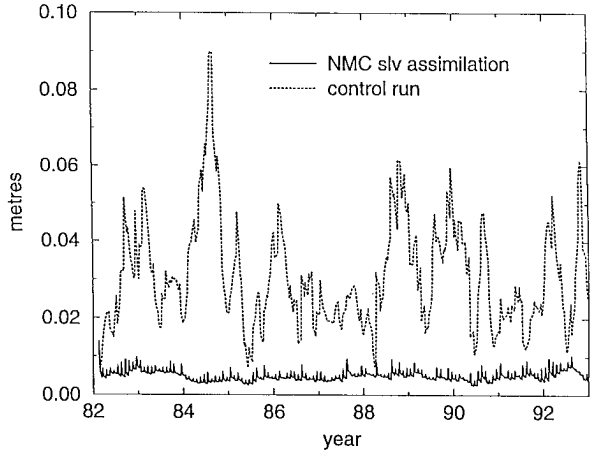

FIG. 6. The rms difference between simulated and NMC reanalysis Nino-4 sea levels with and without assimilation of sea level anomalies.

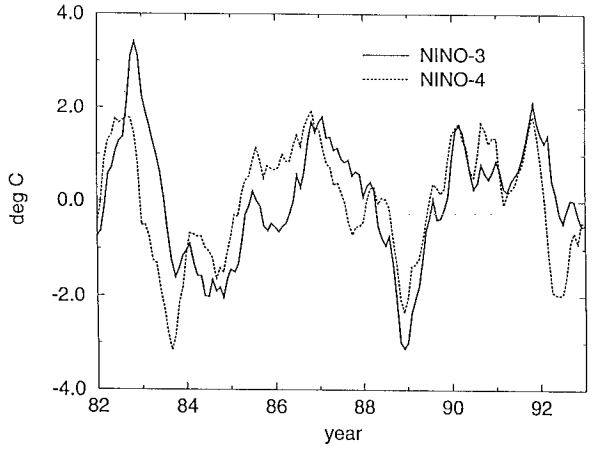

FIG. 7. Temperature anomalies averaged over the upper 275 m, as derived from the sea level assimilation run. The model was forced by observed wind stress data and NMC sea level anomalies were assimilated: (a) control experiment, (b) temperature experiment, (c) sea level experiment.

c. Assimilation of sea level anomalies

The experimental setup is exactly the same as described in the previous section. The model was forced by observed monthly mean FSU wind stress fields, but instead of the temperature monthly mean, NMC sea level anomalies were assimilated during the period February 1982–December 1992. This provides an excellent opportunity to investigate the impact of sea level assimilation on ENSO diagnostics and predictions. Further, it gives an estimate of the potential benefit that can be gained from the insertion of altimetric sea levels. Such data have been available from the Topex/Poseidon and the *ERS-1* missions with good accuracy and high coverage in space and time (Busalacchi et al. 1994; Zou and Burkert 1994).

The rms differences between the NMC sea level anomalies and the model simulations with and without sea level insertion show a reduction in the Nino-4 region by a factor of more than five relative to the control experiment (Fig. 6). Since the simulated sea level anomaly fields are corrected indirectly, this demonstrates that our statistical approach by which we project sea level information onto the vertical temperature structure works successfully. Similar results were found for the Nino-3 region and outside 5°N–5°S. The interannual temperature variability in the sea level assimilation run is increased relative to the control run and even slightly stronger than in the temperature assimilation experiment (Fig. 7). The warm and cold events during the integration period are well simulated. However, during the 1986/87 warm event the temperature drops too early in the Nino-3 region, and too far in the Nino-4 region. The amplitude of our precursor is higher than in the control experiment. From 1982 to 1987, the phase lag between the anomalous heat content in the Nino-3 and Nino-4 regions is clearly seen, and it is more pronounced than in the control experiment. The correlation between monthly mean heat content anomalies in Nino-3 and Nino-4 yields a maximum of 0.75 at a lead time of five months, which is too short relative to observations. However, in contrast to the control experiment the correlation remains at a relatively high level for longer lead times, with a correlation of 0.68 at 12 months lead time. Beginning with the end of the 1986/87 El Niño, this phase lag does not exist any longer, which is in strong contrast to the observations (cf. Fig. 1). The reason for this failure is not understood. One possibility is that the relationship between the sea level and corresponding temperature anomalies changed during that period, which would be harmful to our statistical procedure. However, we did not find clear evidence for this. Another explanation could be that a decadal mode with a period of about 20 years is superimposed on the ENSO cycle, which cannot be simulated by our model. This mode is described by Latif and Barnett 1994, and their hypothesis is that the oscillatory nature of this mode arises from an instability of the coupled ocean–atmosphere system in the North Pacific, which is outside our model domain. Such a mode would change the relationship between anomalous sea levels and corresponding temperatures. If such a decadal mode plays an important role during the late eighties and early nineties, it is plausible that we cannot expect a proper simulation of heat content anomalies for that period. To clarify this, similar experiments will be repeated with a model that includes the North Pacific.

5. Forecast experiments

Recently, different groups have shown that the assimilation of subsurface temperature data may have a positive impact on the skill of ENSO forecasting systems (Ji and Leetmaa 1997; Kleeman et al. 1995). In this

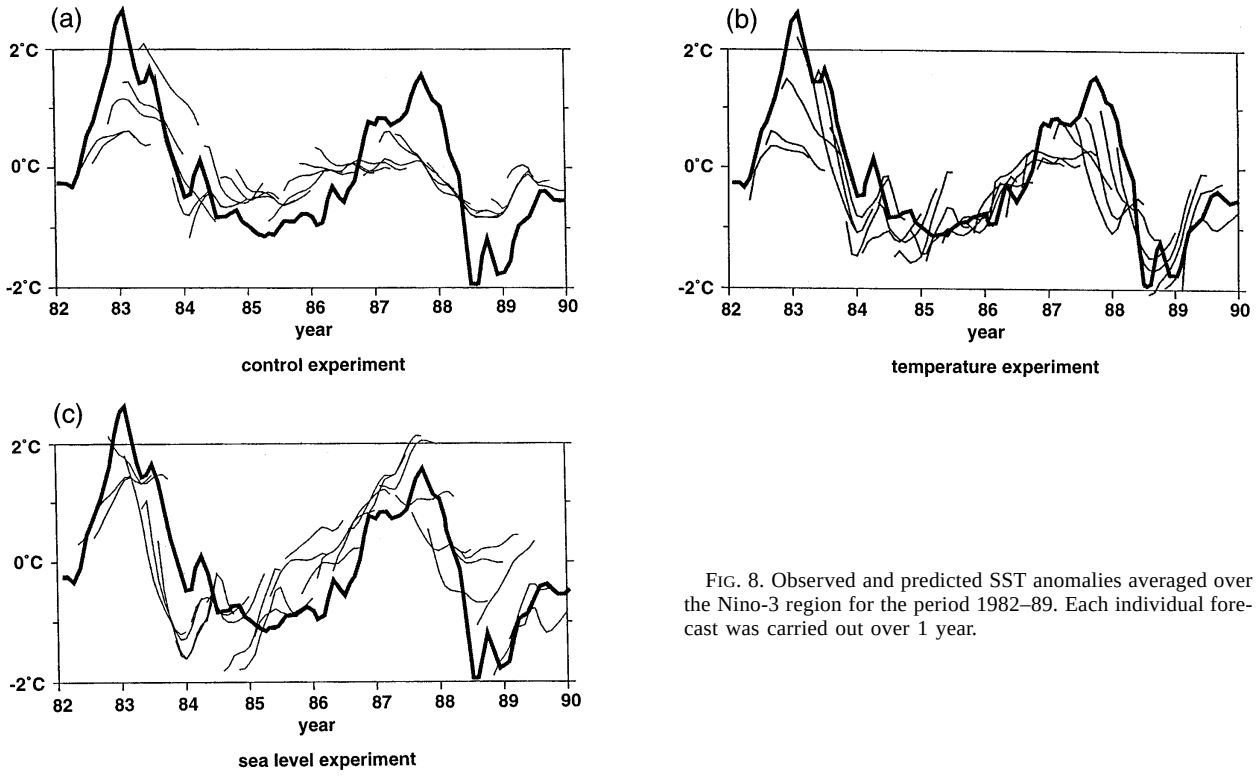

FIG. 8. Observed and predicted SST anomalies averaged over the Nino-3 region for the period 1982–89. Each individual forecast was carried out over 1 year.

section, we present three ensembles of forecast experiments: predictions started from initial states that were obtained from our control run (no data assimilation), from the temperature assimilation run, and from the sea level assimilation run. The forecast integrations were performed with the hybrid coupled model, described in section 2. Each forecast was carried out as follows. To initialize the coupled forecast system, the ocean model was integrated in an uncoupled mode and forced by observed wind stresses. This was done for at least one year, to ensure that the ocean model was properly preconditioned. In a reference ensemble, no additional data were used during the initialization, whereas in the other initialization runs, either monthly mean temperature or sea level anomalies were assimilated. States were stored from each initialization run and used as initial conditions for the hybrid coupled model. The individual forecasts of the SST anomalies in the Nino-3 region and the corresponding observations are presented for the period January 1982–December 1989 in Fig. 8. Beginning in early 1990, the predictive skill of our model drops substantially (not shown). As mentioned in the previous section, the reason for this degradation of the performance partly may be caused by interdecadal climate variability. However, this is not well understood and other groups (U.S. Department of Commerce 1995) also suffer from a similar lack in predictive skill during the 1990s. We therefore decided to restrict the discussion of the forecast results to the period 1982–89. The observed SST anomalies were computed from the Reynolds dataset (Reynolds 1988; Reynolds and Smith 1994) and were not used in any of the initialization experiments.

An objective measure that is commonly used to evaluate the performance of a forecast system is the correlation skill. In our case this measure is based on the correlation between the observed and predicted sea surface temperature anomalies averaged over the Nino-3 region:

$$r(\tau) = \frac{\langle T'_{\text{pred}}(\tau) T'_{\text{obs}}(\tau) \rangle}{[\langle T'_{\text{pred}}(\tau) T'_{\text{pred}}(\tau) \rangle \langle T'_{\text{obs}}(\tau) T'_{\text{obs}}(\tau) \rangle]^{1/2}}. \quad (11)$$

In this equation, $T'_{\text{pred}}(\tau)$ and $T'_{\text{obs}}(\tau)$ denote the predicted and observed SST anomalies, respectively, averaged over the Nino-3 region. The lead time is denoted by τ, and angle brackets denote the forecast ensemble average.

Although the variability of the predicted SST anomalies is too small in the control ensemble (Fig. 8a), the predictive skill is quite good (Fig. 9a). In particular, the transition from warm to cold conditions is predicted well, even at long lead times. Further, no event was erroneously predicted. The forecast skill starts at about 0.75 at lag 0 and remains at a relatively high level even at a lead time of one year (Fig. 9a). However, the 1986/87 warm event was not predicted, even at short lead times. The coupled model simulates warm condi-

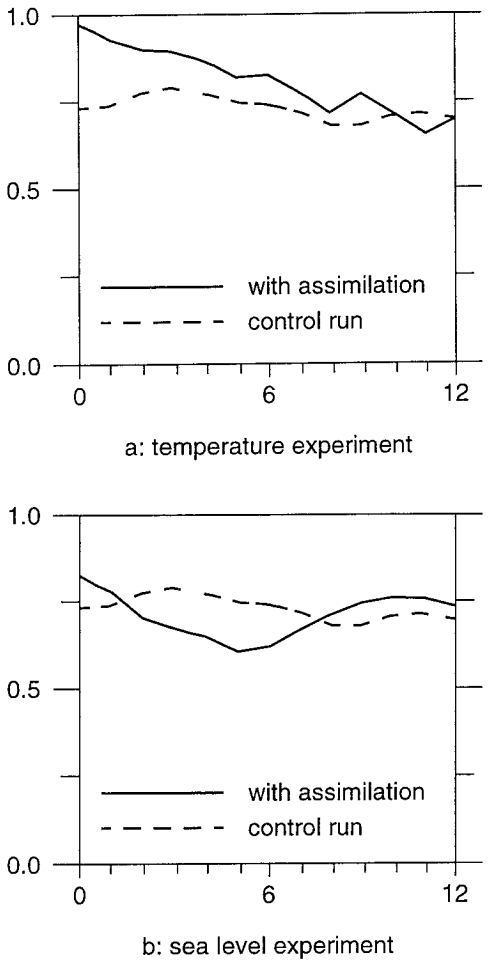

FIG. 9. Forecast skill for sea surface temperature anomalies in Nino-3 averaged over 28 individual forecasts initialized between February 1982 and December 1989.

tions only after the warm event is fully developed in early 1987. Further, the coupled model has some difficulties to simulate the transition from cold or normal to warm conditions in its present configuration. If subsurface temperatures are assimilated during the initialization, the situation improves considerably (Fig. 8b) and the amplitudes of the predicted temperature variations are quite realistic representations. The transition from warm to cold conditions is still well forecasted, and the agreement between observed and predicted SST anomalies is much better between January 1985 and July 1986, a period when the temperature increased continuously. However, the onset of the El Niño 1986/87 is still not very well predicted. Warm conditions are simulated only after the event is fully developed, and even during the height of the 1986/87 warm event, the model is not able to maintain the anomalous conditions and tends to move too early into a cold state. The correlation skill (Fig. 9a) shows clearly that the assimilation of the subsurface temperature anomalies was useful in improving the performance of the forecast system. The correlation skill amounts to about 0.9 at zero lag and reaches the same level as in the control experiment after about one year. This confirms the results of other groups (Ji and Leetmaa 1997; Kleeman et al. 1995), who also found that the use of subsurface information may improve the predictive skill.

The individual forecasts started from the initial conditions obtained from the sea level assimilation experiment are presented in Fig. 8c. Again, the predicted SST variability is more realistic than in the control experiment, although the amplitudes are now bigger than observed. In contrast to the other two forecast ensembles, the 1986/87 El Niño is clearly predicted at lead times up to 1 year. Further, the coupled model remains in a warm state until autumn 1987, which agrees much better with the observations than the results from the previous two ensembles. The strong El Niño in 1982/83 is also predicted better than in the two other ensembles. Weaknesses are found in the temperatures predicted in late 1983 and early 1984. Temperatures are much too cold and the transition from warm to cold conditions is generally predicted poorly relative to the two other forecast ensembles. After the warm event 1986/87 the forecast skill drops substantially, which coincides with the disappearance of the phase lag between the Nino-3 and Nino-4 heat content signals. However, at least from a subjective point of view, the forecasts have gained a lot by assimilating sea level anomalies. Unfortunately, this impression is not confirmed by the correlation skills. Figure 9b shows that the correlation starts at a level slightly higher than in the control ensemble, but it drops below the skill of the control ensemble at lead times between 2 and 7 months. At lead times longer than 7 months the skill is again higher than in the control ensemble.

Comparing the individual forecasts, it is noticeable that in the sea level ensemble the predicted temperature trends are quite realistic. They agree well with observations, even if the forecast itself is quite poor. An example is the prediction that starts in July 1985 (Fig. 8c). The prediction starts at neutral conditions (i.e, SST anomaly of 0°C) and for July 1986 a temperature anomaly of about 1°C is predicted. The corresponding observations are a negative temperature anomaly of about 1°C in July 1985 and almost neutral conditions one year later, which means that the forecast failed completely. However, the observed temperature difference between July 1985 and July 1986 is about 1°C, which also is predicted quite realistically. In the sea level forecast ensemble there are many other examples like this. An objective measure that evaluates the capability to predict trends is the correlation between differences. In our case, we define an alternative skill measure by computing the correlation between the observed and forecasted temperature differences as a function of lead time:

$$s(\tau) = \frac{\langle \Delta T'_{\text{pred}}(\tau)\Delta T'_{\text{obs}}(\tau)\rangle}{[\langle \Delta T'_{\text{pred}}(\tau)\Delta T'_{\text{pred}}(\tau)\rangle\langle \Delta T'_{\text{obs}}(\tau)\Delta T'_{\text{obs}}(\tau)\rangle]^{1/2}}, \quad (12)$$

where $\Delta T'_{\text{pred}}(\tau)$ and $\Delta T'_{\text{obs}}(\tau)$ are the differences between the temperature anomaly at a certain lead time τ minus the temperature anomaly at the initialization time τ_0 as predicted or observed, respectively, and

$$\Delta T'(\tau) = T'(\tau) - T'(\tau_0). \quad (13)$$

Here, $T'_{\text{pred}}(\tau_0)$ and $T'_{\text{obs}}(\tau_0)$ denote the predicted (pred) or observed (obs) temperature anomaly at the initialization time. At short lead times this measure captures only the high-frequency SST fluctuations. These are governed by high-frequency atmospheric noise, and we cannot expect to predict them successfully. Therefore, we do not expect high skills at short lead times using this measure. At medium and long lead times, however, this alternative skill measure should increase if our forecasts capture the low-frequency SST evolution. The alternative skills based on the temperature differences are shown in Fig. 10. In the upper panel, we compare the control ensemble with the temperature assimilation ensemble. They start at about the same level at lag 0. For lead times longer than 3 months, the temperature assimilation ensemble clearly outperforms the control ensemble. The alternative skill measure for the sea level assimilation ensemble (lower panel) starts at a rather low level at lag 0. However, after lead times of about three months the alternative skill of the sea level assimilation ensemble reaches the level of the control ensemble and after 12 months it does even better than the temperature assimilation ensemble.

We conclude that the prediction of the low-frequency component of the tropical Pacific SST anomalies can be improved by assimilating sea level anomalies. Further, both skill measures suggest that the benefit of sea level data is comparable to that of subsurface temperature observations at relatively long lead times of 6–12 months.

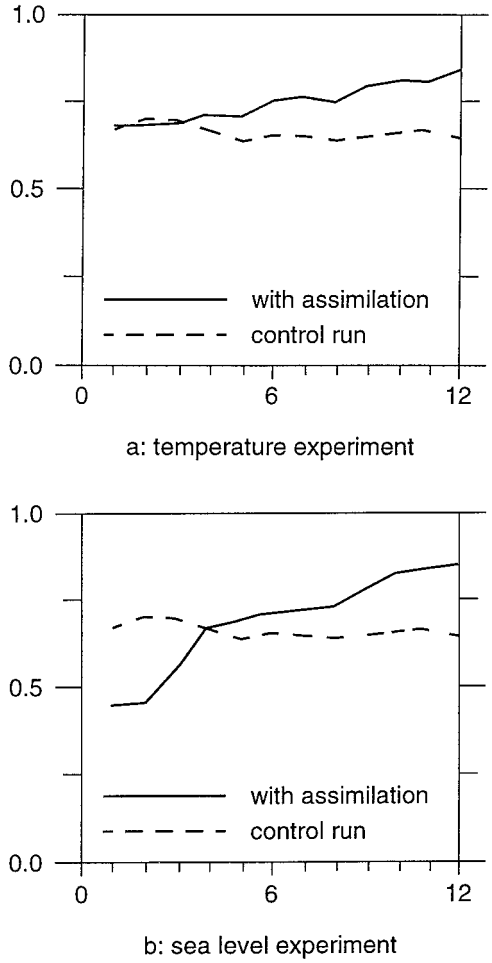

FIG. 10. Forecast skill for differences of sea surface temperature anomalies in Nino-3, as a function of time lag averaged over 28 individual forecasts initialized between February 1982 and December 1989.

6. Conclusions

We have investigated the potential impact of sea level assimilation on ENSO simulations and forecasts. An empirical scheme was developed by which the sea level anomalies can be projected onto the anomalous vertical density structure of the ocean. It was shown that the assimilation of both subsurface temperature and sea level anomalies improves the simulation of the ocean states, especially in the western equatorial Pacific, which is a crucial region for ENSO predictions.

The results of the forecast ensembles indicate that the assimilation of sea level anomalies yields comparable results to the case in which subsurface temperature anomalies were assimilated. Thus, we can expect a positive impact on ENSO forecasting by assimilating altimetric sea level anomalies. Such data are currently available in near real time and have the advantage of high spatial and temporal resolution. Preliminary forecast results using altimetric height anomalies are also encouraging (Fischer et al. 1994).

Our study indicates also that the question of forecast verification needs to be addressed in more detail. We have shown that the interpretation of the forecast result critically depends on the definition of the skill measure. The positive impact of data assimilation on ENSO predictions could be shown more clearly when the forecasted temperature anomaly differences rather than the temperature anomalies themselves were compared with observations. Furthermore, based on the subjective impression, the forecasts with sea level data assimilation looked much more realistic than those without data assimilation, which was not supported by the traditional skill measure. However, further work is needed to understand this in more detail.

Acknowledgments. This work was supported by ESTEC under Grant 144293 and by the German WOCE

program. The computations were performed at the Deutsches Klima Rechenzentrum in Hamburg. The authors would also like to thank the reviewers for their helpful comments on the manuscript.

REFERENCES

Barnett, T. P., N. E. Graham, M. A. Cane, S. E. Zebiak, S. C. Dolan, J. J. O'Brien, and D. Legler, 1988: On the prediction of the El Niño 1986/87. *Science,* **241,** 192–196.

——, M. Latif, N. Graham, M. Flügel, S. Pazan, and W. White, 1993: ENSO and ENSO related predictability. Part 1: Prediction of equatorial Pacific sea surface temperature with a hybrid coupled ocean–atmosphere model. *J. Climate,* **6,** 1545–1566.

Busalacchi, A., M. J. McPhaden, and J. Picaut, 1994: Variability in equatorial Pacific sea surface topography during the verification phase of the TOPEX/POSEIDON mission. *J. Geophys. Res.,* **99**(C12), 24 725–24 738.

Cane, M. A., S. E. Zebiak, and S. C. Dolan, 1986: Experimental forecasts of El Niño. *Nature,* **321,** 827–832.

Daley, R., 1991: *Atmospheric Data Analysis.* Cambridge University Press, 457 pp.

Fischer, M., and M. Latif, 1995: Assimilation of temperature and sea level observations into a primitive equation model of the tropical Pacific. *J. Mar. Syst.,* **6,** 31–46.

——, ——, M. Flügel, and J. Zou, 1994: Assimilation of sea level data into a primitive equation model of the tropical Pacific. TOGA Notes 1–5. [Available from Nova Southeastern University, Oceanographic Center, 8000 North Ocean Drive, Dania, FL 33004.]

Goldenberg, S. O., and J. J. O'Brien, 1981: Time and space variability of tropical Pacific wind stress. *Mon. Wea. Rev.,* **109,** 1190–1207.

Haney, R. H., 1971: Surface thermal boundary conditions for ocean circulation models. *J. Phys. Oceanogr.,* **1,** 241–248.

Ji, M., and A. Leetmaa, 1997: Impact of data assimilation on ocean initialization and El Niño prediction. *Mon. Wea. Rev.,* **125,** 742–753.

——, A. Kumar, and A. Leetmaa, 1994: An experimental coupled forecast system at the National Meteorological Center: Some early results. *Tellus,* **46A,** 398–418.

——, A. Leetmaa and J. Derber, 1995: An ocean analysis system for seasonal to interannual climate studies. *Mon. Wea. Rev.,* **123,** 460–481.

Kleeman, R., A. M. Moore, and N. R. Smith, 1995: Assimilation of subsurface thermal data into a simple ocean model for the initialization of an intermediate tropical coupled ocean–atmosphere forecast model. *Mon. Wea. Rev.,* **123,** 3103–3113.

Latif, M., 1987: Tropical ocean circulation experiments. *J. Phys. Oceanogr.,* **17,** 246–263.

——, T. P. Barnett, 1994: Causes of decadal climate variability over the North Pacific and North America. *Science,* **226,** 634–637.

——, ——, M. A. Cane, N. E. Graham, H. von Storch, J.-S. Xu, and S. E. Zebiak, 1994: A review of ENSO prediction studies. *Climate Dyn.,* **9,** 167–179.

Leetmaa, A., and M. Ji, 1989: Operational hindcasting of the tropical Pacific. *Dyn. Atmos. Oceans,* **13,** 465–490.

Legler, D. M., and J. J. O'Brien, 1984: *Atlas of Tropical Pacific Wind Stress Climatology 1971–1980.* The Florida State University Press, 182 pp.

Levitus, S., and R. D. Gelfeld, 1992: National Oceanographic Data Center, inventory of physical oceanographic profiles, global distribution by year for all countries. NOAA, Key to Oceanographic Records Documentation No. 18, US Department of Commerce. [Available from U.S. Department of Commerce, National Oceanographic Data Center, User Service Branch, NOAA/NESDIS, E/OC21, Washington, D.C. 20235.]

Mellor, G. L., and T. Ezer, 1991: A Gulf Stream model and an altimetry assimilation scheme. *J. Geophys. Res.,* **96,** 8779–8795.

Neelin, J. D., M. Latif, and F.-F. Jin, 1994: Dynamics of coupled ocean–atmosphere models: The tropical problem. *Annu. Rev. Fluid Mech.,* **26,** 617–659.

Pacanowski, R. C., and S. G. H. Philander, 1981: Parameterization of vertical mixing in numerical models of tropical oceans. *J. Phys. Oceanogr.,* **11,** 632–645.

Reynolds, R. W., 1988: A real time global sea surface temperature analysis. *J. Climate,* **1,** 75–86.

——, and T. M. Smith, 1994: Improved global sea surface temperature analysis using optimal interpolation. *J. Climate,* **7,** 929–948.

Ropelewski, C. F., and M. S. Halpert, 1987: Global and regional scale precipitation patterns associated with the El Niño/Southern Oscillation. *Mon. Wea. Rev.,* **115,** 1606–1626.

Schopf, P. S., and M. J. Suarez, 1988: Vacillations in a coupled ocean–atmosphere model. *J. Atmos. Sci.,* **45,** 549–566.

U.S. Department of Commerce, 1995: Climate Diagnostics Bulletin 95/4, 46–54, 78 pp. [Available from Climate Analysis Center, W/NMC52, NOAA/NWS/NMC, NOAA Science Research Center, Room 605, 5200 Auth Rd., Washington, D.C. 20233.]

Wyrtki, K., 1988: Water displacements in the Pacific and the genesis of El Niño cycles. *J. Geophys. Res.,* **90**(C4), 7129–7132.

Zou, J., and R. Burkert, 1994: Sea level variations in the tropical Pacific during 1992–1993 derived from ERS-1 altimetry. *Proc. Second ERS-1 Symp.,* Hamburg, Germany ESA, 519–522.